Am J Cardiovasc Dis 2022;12(4):205-211
www.AJCD.us /ISSN:2160-200X/AJCD0144645

Original Article

Early reversibility of histological changes after experimental acute cardiac volume-overload

Christa Huuskonen[1], Mari Hämäläinen[2], Nooa Kivikangas[1], Timo Paavonen[3], Eeva Moilanen[2], Ari A Mennander[1]

[1]Tampere University Heart Hospital and Faculty of Medicine and Health Technology, Tampere University, Tampere, Finland; [2]The Immunopharmacology Research Group, Faculty of Medicine and Health Technology, Tampere University and Tampere University Hospital, Tampere, Finland; [3]Department of Pathology, Fimlab, Tampere University Hospital and Faculty of Medicine and Health Technology, Tampere, Finland

Received June 9, 2022; Accepted August 15, 2022; Epub August 15, 2022; Published August 30, 2022

Abstract: Unloading the heart may aid recovery after acute cardiac volume-overload (AVO). We experimentally investigated whether unloading the heart after AVO by heterotopic transplantation histologically impacts myocardial outcome. Thirty-two syngeneic Fisher 344 rats underwent surgery for abdominal arterial-venous fistula to induce AVO. Seven hearts were heterotopically transplanted one day after AVO to simulate a non-working state of the left ventricle (AVO+Tx). In addition, six rats without AVO or surgery (Normal) and five rats with sham surgery (Sham) served as controls. Myocardial outcome was studied using histology and quantitative reverse-transcription polymerase chain reaction (qRT-PCR) analysis for hypoxia inducible factor 1alpha (HIF1α), inducible nitric oxide synthase (iNOS), E-selectin, atrial natriuretic peptide (ANP), brain natriuretic peptide (BNP), vascular endothelial growth factor alpha (VEGFα), matrix metalloprotease 9 (MMP9), chitinase-3-like protein (YKL-40) and transforming growth factor beta (TGFβ). Relative ischemia of the right ventricle and septal intramyocardial arteries was decreased in AVO+Tx as compared with AVO (0.04±0.01 vs. 0.09±0.02, PSU, *P*=0.040 and 0.04±0.01 vs. 0.16±0.02, PSU, P=0.008, respectively). Quantitative RT-PCR showed an increase in the expression of iNOS, YKL-40 and VEGFα, and decrease in ANP in AVO+Tx as compared with AVO (5.78±1.23 vs. 2.46±0.81, *P*=0.039, 22.39±5.22 vs. 10.79±1.70, *P*=0.039 and 1.15±0.22 vs. 0.60±0.08, *P*=0.030, and 1.32±0.16 vs. 2.85±0.70, *P*=0.039, respectively). Unloading the heart by heterotopic transplantation induces early ischemic recovery of intramyocardial arteries after AVO. A non-working state reverses acute ischemic myocardial injury after AVO.

Keywords: Acute volume-overload (AVO), heterotopic rat cardiac transplantation, ischemia, intramyocardial artery

Introduction

Healthy blood circulation includes venous blood return in a low-pressurized fashion via the vena cava to the right side of the heart. A sudden traumatic connection of the aorta and vena cava allows pressurized arterial blood to fill the vena cava excessively, thereby creating an acute volume-overload (AVO) of the right side of the heart. The excessive acute blood flow into the heart increases the functional working-load of the heart as well as myocardial oxygen consumption. Irreversible cardiac tissue damage may ensue after AVO despite early surgery [1]. AVO of the heart is a clinical emergency occurring after tricuspid valve regurgitation, atrial or ventricular rupture of the cardiac septum or rupture of the aortic root to the right atrium, leading to increased cardiac oxygen consumption and early ischemic-like changes in the myocardium [1, 2]. To release cardiac stress and to enable salvage surgery in the acute phase of AVO, it is indispensable to reduce circulatory afterload. A mechanical assist device may compensate heart function in overtaking some of the excessive work during acute volume-overload. A left ventricular assist device (LVAD) may be applied for hemodynamic aid to unload the heart, but early reversibility of the myocardial changes due to AVO remains unknown [3, 4].

We have previously shown that AVO of rat hearts induces early ischemia of intramyocardial arter-

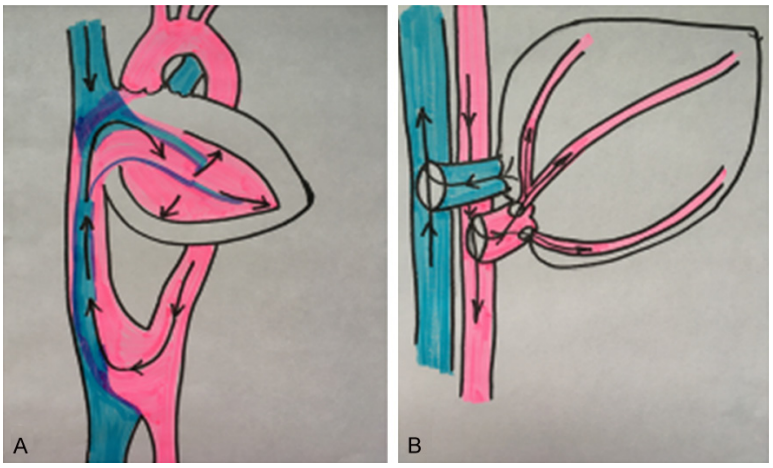

Figure 1. A. Schematic illustration of a heart during acute volume-overload (AVO). The intra-abdominal aorta and inferior vena cava are anastomosed to create a 5 mm long aorto-venous fistula. Arrows indicate main direction of blood circulation in main vessels and increased filling of the right side of the heart. Pink and blue colors indicate oxygenated and deoxygenated blood, respectively. B. Schematic illustration of a heterotopically transplanted heart after acute volume-overload (AVO+Tx). Hearts with acute volume-overload were transplanted intra-abdominally by anastomosing the graft aorta to the abdominal aorta and the graft pulmonary artery to the inferior vena cava of the recipient, respectively. Arrows indicate main direction of blood circulation in main vessels and coronary arteries of the graft. Due to the presence of competent aortic and pulmonary valves, the heart is unloaded as the left atrial filling is avoided. Pink and blue colors indicate oxygenated and deoxygenated blood, respectively.

ies throughout the whole heart, encompassing the right and left ventricle as well as the septum [2]. In this study, syngeneic rat hearts with AVO were further heterotopically transplanted to simulate a LVAD, and early myocardial histology was studied after a 30-min unloaded state of the transplanted heart. Gene expressions of selected markers were investigated to delineate plausible effect of the unloaded heart state: atrial natriuretic peptide (ANP) and brain natriuretic peptide (BNP) mirror compensation of congestive heart failure [5], hypoxia-inducible factor 1alpha (HIF1α) and inducible nitric oxide synthase (iNOS) serve as markers for oxygen exchange [6, 7], E-selectin for inflammation [8], vascular endothelial growth factor alpha (VEGFα) for angiogenesis [9], matrix metalloproteinase 9 (MMP9) and transforming growth factor beta (TGFβ) for cardiac remodeling [10, 11], and chitinase-3-like protein (YKL-40) for inflammation, inhibition of apoptosis, and cardiac remodeling [12]. The aim of the present study was to experimentally investigate whether a non-working state of the heart impacts intramyocardial ischemia due to AVO.

Material and methods

Rats

The rats were randomly assigned in groups. An abdominal aorta-vena cava fistula was surgically created in 32 Fischer-344 male rats (F344/NHsd, Harlan Laboratories, The Netherlands) weighing 200-350 g to create AVO as described previously [2]. One day after surgery, seven hearts with AVO were heterotopically transplanted (AVO+Tx) to obtain a non-working cardiac graft simulating a left ventricle assisting device. Five rats were sham-operated (Sham) by opening the abdominal cavity and temporarily clamping the inferior vena cava and the abdominal aorta for 15 min without creating AVO, and six unoperated rats served as Normal. The rats were kept in Tampere University vivarium and received humane care in compliance with the "Principles of Laboratory Animal Care" formulated by the National Society for Medical Research and the "Guide for the Care and Use of Laboratory Animals" prepared by the Institute of Laboratory Animal Resources and published by the National Institutes of Health (NIH publication No. 86-23, revised 1996). The study was approved by the Finnish State Provincial Office.

Surgical procedure

The rats were anesthetized with sevoflurane (Baxter, USA) for inhalation and pentobarbiturate (Mebunat vet®; Orion Espoo, Finland; 50 mg/kg) intraperitoneally. The abdominal cavity was surgically opened, and the inferior vena cava and the aorta were exposed. An aorto-venous fistula was performed by vertically incising 5 mm the abdominal aorta as well as the adjacent inferior vena cava while joining these vessels surgically with a 7-0 running vascular suture. 100 U Heparin Leo, (Vianex S.A., Greece) was administered intravenously (**Figure 1A**). After creation of the arteriovenous fistula,

the pulsation of arterial blood was palpated on the vena cava; the 5-mm-long arteriovenous surgical connection enabled a visual increase in blood flow and surge of clear red arterial blood to the vena cava immediately after suture of the fistula, thus confirming the acute increase in circulating blood flow and volume-overload. One day after AVO, seven cardiac grafts were harvested after an immediate 4°C infusion of cold physiologic saline fluid into the aorta and kept cold. Thereafter, heterotopic cardiac transplantation was performed as previously described [13, 14]. Briefly, heterotopic cardiac transplantation was performed intra-abdominally by joining the graft aorta to the abdominal aorta and the graft pulmonary artery to the inferior vena cava of the recipient, respectively (**Figure 1B**). The cardiac graft received oxygenated blood from the recipient abdominal aorta via the coronary arteries of the graft. Through the coronary sinus, right atrium, right ventricle and pulmonary artery, blood recirculated back to the recipient rat. Since the aortic valve was competent, oxygenated blood was not allowed to fill the left ventricle and, therefore, the transplanted heart simulated a non-working resting state of the left side of the graft [13]. Visual inspection revealed color change of the heart from dark brown to light beige in addition to strong heart pulsation, thus confirming successful transplantation surgery. After the procedure, buprenorfin (Vetergesic®; Orion Espoo, Finland; 0.1 mg/100 g) and carprofen (Norocarp®; Norbrook Laboratories Limited, Newry, Northern Ireland; 0.5 mg/100 g) were administered subcutaneously for pain relief.

Tissue samples

The rats were sacrificed one day after surgery (AVO, Sham). The rats with AVO+Tx were sacrificed 30 min after transplantation, thereby allowing a 30-min non-working state of the heart with AVO. The basal part of the hearts was stored in RNAlater® (Applied Biosystems, CA, USA) for quantitative RT-PCR analysis. The apex part of the heart was fixed in formalin and embedded in paraffin.

Histology

For histology, 5 µm sections were cut and stained with Haematoxylin and Eosin. Presence of myocardial edema, ischemia and inflammation was evaluated and graded according to an arbitrary scale from 0 (no edema, ischemia, or inflammation) to 1 (presence of edema, ischemia, or inflammation). Representative cross-sectional intramyocardial arteries were chosen randomly from the right and left ventricular walls and the septum. Normal, vacuolated and sharp-edged media cell nuclei of the intramyocardial arteries were investigated and recorded. The relative number of ischemic nuclei of intramyocardial arteries was calculated by dividing the total number of sharp-edged media cell nuclei by the normal round-shaped nuclei. The relative number of vacuolated nuclei of intramyocardial arteries was calculated by dividing the total number of vacuolated media cell nuclei by the normal round-shaped nuclei. The evaluation of histology was performed blinded to the study protocol by two investigators (CH, AM).

Quantitative RT-PCR analysis

The base of the heart was homogenized and RNA extraction was carried out with an RNeasy mini kit with on-column DNase digestion (Qiagen, Hilden, Germany), and total RNA was then reverse-transcribed to cDNA using Maxima First Strand cDNA synthesis kit (Thermo Fisher Scientific, Waltham, MA, USA). The cDNA obtained from the RT reaction (amount corresponding to approximately 1 ng of total RNA) was subjected to quantitative PCR using QuantiTect® Primer Assays (Qiagen, Valencia, CA, USA) for HIF1α, iNOS, E-selectin, ANP, BNP, VEGFα, MMP9, YKL-40, TGFβ and GAPDH, Maxima® SYBR Green/ROX qPCR Master Mix (Thermo Scientific, Waltham, MA, USA) and ABI PRISM 7000 Sequence detection system (Applied Biosystems, Foster City, CA, USA). PCR reaction parameters for SYBR® Green detection were as follows: incubation at 50°C for two minutes, incubation at 95°C for 10 minutes, and thereafter 40 cycles of denaturation at 95°C for 15 seconds, and annealing and extension at 60°C for one minute. Each sample was determined in duplicate. Ct values were determined, and the relative quantification was calculated using the $2^{-\Delta\Delta Ct}$ method [15]. The values of six control samples (Normal) were used as a calibrator, and the expression levels of HIF1α, iNOS, E-selectin, ANP, BNP, VEGFα, MMP9, YKL-40 and TGFβ were normalized against GAPDH.

Immunohistochemistry

Immunohistochemistry was performed using the Ventana Life-sciences Benchmark XT©

Table 1. Early histology of medial cell nuclei of intramyocardial arteries of unoperated hearts (Normal), sham-operated hearts (Sham), hearts with acute volume-overload (AVO) and heterotopically transplanted heart after AVO (AVO+Tx)

	Normal	Sham	AVO	AVO+Tx	Mann-Whitney U test *P*-value	Kruskall-Wallis test *P*-value
Right ventricle						
Relative number of ischemic nuclei	0.05±0.02	0.07±0.01	0.09±0.02	0.04±0.01	0.040*	0.149
Relative number of vacuolated nuclei	0.10±0.04	0.07±0.02	0.12±0.02	0.07±0.02	0.493	0.902
Left ventricle						
Relative number of ischemic nuclei	0.04±0.01	0.11±0.03	0.09±0.02	0.03±0.01	0.069	0.042*
Relative number of vacuolated nuclei	0.12±0.05	0.09±0.03	0.12±0.05	0.30±0.05	0.002*	0.010*
Septum						
Relative number of ischemic nuclei	0.03±0.01	0.10±0.02	0.16±0.02	0.04±0.01	0.008*	0.001*
Relative number of vacuolated nuclei	0.10±0.04	0.06±0.06	0.18±0.04	0.14±0.05	0.946	0.260

Values are expressed as mean ± error of mean; Mann-Whitney U test comparing AVO vs. AVO+Tx. *P<0.05.

Staining module. The paraffin-embedded slides were deparaffinized with three changes of xylene, rehydrated in a series of graded ethanol, and rinsed well under running distilled water. The slides were placed in a preheated retrieval buffer, 0.1 mmol EDTA, pH 8.0, for 30 min and then cooled in a buffer for 5 min, followed by a 5-minute rinse under running distilled water. After heat-induced epitope retrieval, the slides were placed on an autostainer (DAKO Corp., Carpinteria, CA, USA). Sections were incubated with 3% hydrogen peroxide in ethanol for 5 min to inactivate the endogenous peroxides, and incubated in YKL-40 antibody (dilution 1:100) (Biomedica Gruppe) for 30 min, followed by rinsing with Tris-buffered saline solution with Tween 20 (TBST) wash buffer. Secondary incubation was made using DUAL-labeled polymer horseradish peroxidase (K4061; DAKO Corp.) for 15 min. The slides were rinsed with TBST wash buffer. Sections were then incubated in 3,3'-diaminobenzidine (K3467; DAKO Corp.) for 5 min, counterstained with modified Schmidt hematoxylin for 5 min, rinsed for 3 min in tap water to blue sections, dehydrated with graded alcohols, and cleared in three changes of xylene before mounting. Positively stained YKL-40 cells were evaluated from representative cross-sectional area samples of the right ventricular wall, the left ventricular wall, and the septum. The evaluation was performed by two investigators blinded to the study protocol (NK, AM).

Statistical analysis

The data is presented as mean ± standard error of mean (SEM). Statistical analyses were performed with SPSS 26.0 statistical software (SPSS Inc, Chicago, IL). Nonparametric data between the groups were analyzed with Kruskall-Wallis and Mann-Whitney U test. The *P*-values <0.05 were considered significant.

Results

Histology

The presence of myocardial edema, ischemia and inflammation did not differ between the groups.

Relative number of ischemic nuclei of the right ventricle, left ventricle and septal intramyocardial arteries was decreased in AVO+Tx as compared with AVO (0.04±0.01 vs. 0.09±0.02, PSU, *P*=0.040; 0.03±0.01 vs. 0.09±0.02, PSU, *P*=0.069 and 0.04±0.01 vs. 0.16±0.02, PSU, *P*=0.008, respectively, **Table 1**). Relative number of vacuolated nuclei of the right ventricle and septal intramyocardial arteries did not differ between the groups. The relative number of vacuolated nuclei of the left ventricle intramyocardial arteries was increased in AVO+Tx as compared with AVO (0.30±0.05 vs. 0.12±0.05, PSU, *P*=0.002, **Figure 2**).

qRT-PCR analysis

As presented in **Table 2**, iNOS was upregulated more than double in AVO+Tx as compared with AVO (5.78±1.23 vs. 2.46±0.81, *P*=0.039), whereas E-selectin showed a tendency of increase in AVO+Tx as compared with AVO (8.82±2.56 vs. 5.08±1.70, *P*=0.051). ANP was downregulated in AVO+Tx as compared with AVO (1.32±0.16 vs. 2.85±0.70, *P*=0.039). Th-

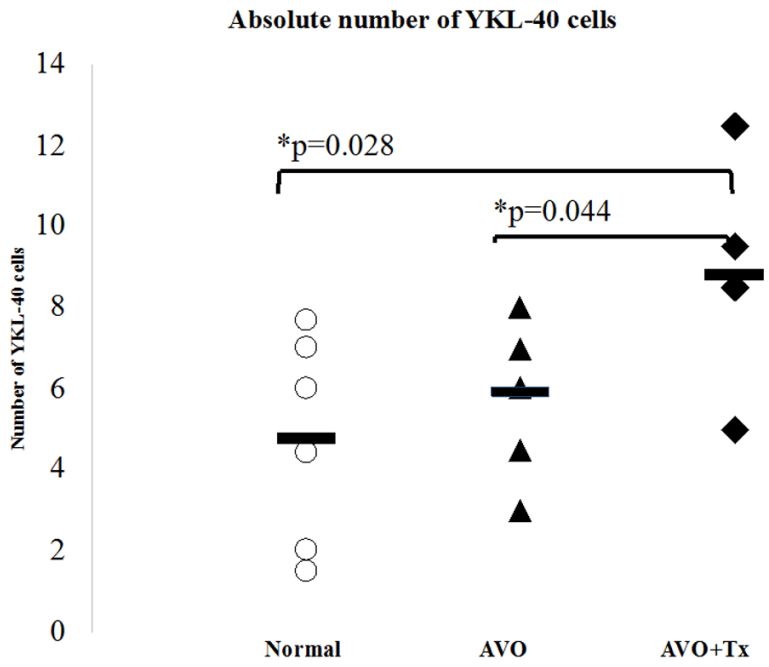

Figure 2. Absolute number of YKL-40 positive myocardial cells in Normal, hearts with acute volume-overload (AVO) and heterotopically transplanted hearts after AVO (AVO+Tx). Horizontal bars indicate mean.

ough VEGFα expression was higher in AVO+Tx as compared with AVO (1.15±0.22 vs. 0.60±0.08, *P*=0.030), it remained at the level of Normal. YKL-40 was upregulated more than double in AVO+Tx as compared with AVO (22.39±5.22 vs. 10.79±1.70, *P*=0.039).

Immunohistochemistry for YKL-40

The absolute number of YKL-40 positive myocardial cells was higher in AVO+Tx vs. AVO (8.80±2.68 vs. 5.92±1.86, *P*=0.044).

Discussion

AVO induces a sudden circulatory burden that causes ischemic-like changes of the myocardium [1, 4]. Intramyocardial arteries are particularly vulnerable to early volume overload and mirror early ischemia-like insult of the myocardium [2]. In this study, we investigated whether a non-working state of the heart would interfere with intramyocardial ischemia after experimental AVO.

The relative number of ischemic nuclei of the right ventricle, left ventricle and septal intramyocardial arteries of hearts with AVO after heterotopic transplantation decreased back to the level of the number observed in untouched normal hearts. The non-working state of the heart after heterotopic transplantation afforded a reversible circulatory burden simulating the application of a LVAD [3]. The relative increase of the number of vacuolated nuclei of the left ventricle intramyocardial arteries in hearts with AVO+Tx may confirm the reversed circulation and the early unloaded effect on the left side of the heart; increased coronary artery circulation after heterotopic cardiac transplantation induces increased myocardial perfusion pressure and intracellular edema, while the left side of the heart remains in the non-working state [16].

The decreased expression of ANP and induced upregulation of iNOS suggest that hypoxic myocardial changes in hearts with AVO interact early after downloading of the circulation [7, 17]. Major differences in the expressions of TGFβ and MMP9 were not observed at the early phase of AVO+Tx as compared with AVO, probably since the induction of TGFβ and MMP9 instead reflect the onset of fibrosis at a later stage after AVO [18]. Both preserved upregulation of VEGFα and increased YKL-40 expressions suggest angiogenesis and compensatory remodeling mechanisms after AVO+Tx [9, 19]. YKL-40 expression and immunohistochemical staining of YKL-40 increased in hearts with AVO+Tx, while in the AVO group they were at the level comparable with untouched normal hearts. YKL-40 is a sensitive marker of inflammation and cardiac remodeling after surgical trauma [12]; YKL-40 induces angiogenesis and has antiapoptotic properties that inhibit inflammation [20].

From a clinical perspective, the heart exerts excessive work against AVO [1, 4]. The resulting hemodynamically unstable acute heart with increased myocardial oxygen consumption is a life-threatening emergency. Indeed, a circulatory support that hemodynamically allows the

Table 2. Gene expression of unoperated hearts (Normal), sham-operated hearts (Sham), hearts with acute volume-overload (AVO) and heterotopically transplanted hearts after AVO (AVO+Tx)

	Normal	Sham	AVO	AVO+Tx	Mann-Whitney U test *P*-value	Kruskall-Wallis test *P*-value
HIF1α	1.00±0.08	1.19±0.06	1.19±0.15	1.32±0.10	0.448	0.157
iNOS	1.00±0.28	1.68±0.25	2.46±0.81	5.78±1.23	0.039*	0.014*
E-selectin	1.00±0.23	2.42±0.29	5.08±1.70	8.82±2.56	0.051	<0.001*
ANP	1.00±0.22	1.67±0.75	2.85±0.70	1.32±0.16	0.039*	0.040*
BNP	1.00±0.70	0.97±0.11	1.33±0.42	1.59±0.45	0.448	0.697
VEGFα	1.00±0.11	2.01±0.15	0.60±0.08	1.15±0.22	0.030*	0.001*
MMP9	1.00±0.39	5.84±2.13	13.61±5.05	4.41±0.90	0.278	0.010*
YKL-40	1.00±0.26	10.46±1.81	10.79±1.70	22.39±5.22	0.039*	<0.001*
TGFβ	1.00±0.12	1.52±0.06	3.33±0.55	2.61±0.15	0.448	0.001*

Gene expression was measured by qRT-PCR and normalized against GAPDH. The mean expression level in the Normal group was set as 1 and the other values are expressed in relation to that value. Values are given as mean ± standard error of mean. Mann-Whitney U test comparing AVO vs. AVO+Tx. Kruskall-Wallis test compares all groups. HIF1α = hypoxia inducible factor 1alpha, iNOS = inducible nitric oxide synthase, ANP = atrial natriuretic peptide, BNP = brain natriuretic peptide, VEGFα = vascular endothelial growth factor alpha, MMP9 = matrix metalloproteinase 9, YKL-40 = chitinase 3-like protein, TGFβ = tumor growth factor beta. *P<0.05.

heart to rest enables a non-working state of the heart with less oxygen consumption, securing patient recovery from surgical correction of the aorta-venous connection [3]. The non-working heart state may also provide reversible myocardial changes after ischemia-like strain caused by AVO. In the future, we aim to study whether the non-working state of the heart after AVO would further enhance reversed tissue remodeling after long-term follow-up time.

The experimental approach of this study cannot compensate the need of clinical investigation of the effect of an LVAD in reversing myocardial changes after AVO. Histologically, however, well-settled *in-vivo* experimental models may serve as a pilot set-up that indicates whether a non-working heart state offers induction of reversed tissue remodeling. The application of an LVAD-type of device after AVO may be a worthy means of treatment to compensate the ongoing ischemia-state of an overloaded heart.

Acknowledgements

This work was supported by research funding from The Competitive State Research Financing of the Expert Responsibility area of Tampere University Hospital and Tuberculosis Foundation. We wish to thank Ms Meiju Kukkonen for excellent technical assistance.

Disclosure of conflict of interest

None.

Address correspondence to: Dr. Ari A Mennander, Tampere University Heart Hospital, SDSKIR, Elämänaukio 1, P.O. Box 2000 Tampere, Finland. E-mail: ari.mennander@sydansairaala.fi

References

[1] Loh E. Maximizing management of patients with decompensated heart failure. Clin Cardiol 2000; 23: III1-III5.

[2] Huuskonen C, Hämäläinen M, Bolkart R, Soininen T, Kähönen V, Paavonen T, Moilanen E and Mennander A. Surgical acute volume-overload impacts early on myocardium-an experimental study. Acta Cardiol Sin 2017; 33: 630-636.

[3] Wohlschlaeger J, Schmitz K, Schmid C, Schmid K, Keul P, Takeda A, Weis S, Levkau B and Baba HA. Reverse remodeling following insertion of left ventricular assist devices (LVAD): a review of the morphological and molecular changes. Cardiovasc Res 2005; 68: 376-386.

[4] Koerner MM, Loebe M, Lisman KA, Stetson SJ, Lafuente JA, Noon GP and Torre-Amione G. New strategies for the management of acute decompensated heart failure. Curr Opin Cardiol 2001; 16: 164-173.

[5] Stumpe KO, Sölle H, Klein H and Krück F. Mechanism of sodium and water retention in rats with experimental heart failure. Kidney Int 1973; 4: 309-317.

[6] Wang T, Liu H, Lian G, Zhang SY, Wang X and Jiang C. HIF1α-induced glycolysis metabolism is essential to the activation of inflammatory macrophages. Mediators Inflamm 2017; 2017: 9029327.
[7] Melillo G, Musso T, Sica A, Taylor LS, Cox GW and Varesio L. A hypoxia-responsive element mediates a novel pathway of activation of the inducible nitric oxide synthase promoter. J Exp Med 1995; 182: 1683-1693.
[8] Leeuwenberg JF, Smeets EF, Neefjes JJ, Shaffer MA, Cinek T, Jeunhomme TM, Ahern TJ and Buurman WA. E-selectin and intercellular adhesion molecule-1 are released by activated human endothelial cells in vitro. Immunology 1992; 77: 543-549.
[9] Banai S, Jaklitsch MT, Shou M, Lazarous DF, Scheinowitz M, Biro S, Epstein SE and Unger EF. Angiogenic-induced enhancement of collateral blood flow to ischemic myocardium by vascular endothelial growth factor in dogs. Circulation 1994; 89; 2183-2189.
[10] Creemers E, Cleutjens J, Smits J and Daemen M. Matrix metalloproteinase inhibition after myocardial infarction. Circ Res 2001; 89: 201-210.
[11] Ellmers LJ, Scott NJ, Medicherla S, Pilbrow AP, Bridgman PG, Yandle T, Richards AM, Protter AA and Cameron VA. Transforming growth factor-β blockade down-regulates the renin-angiotensin system and modifies cardiac remodeling after myocardial infarction. Endocrinology 2008; 149: 5828-5834.
[12] Tiriveedhi V, Upadhya GA, Busch RA, Gunter KL, Dines JN, Knolhoff BL, Jia J, Sarma NJ, Ramachandran S, Anderson CD, Mohanakumar T and Chapman WC. Protective role of bortezomib in steatotic liver ischemia/reperfusion injury through abrogation of MMP activation and YKL-40 expression. Transpl Immunol 2014; 30: 93-98.
[13] Suzuki K, Murtuza B, Smolenski RT, Suzuki N and Yacoub MH. Development of an in vivo ischemia-reperfusion model in heterotopically transplanted rat hearts. Transplantation 2002; 73: 1398-1402.
[14] Vuohelainen V, Raitoharju E, Levula M, Lehtimaki T, Pelto-Huikko M, Honkanen T, Huovila A, Paavonen T, Tarkka M and Mennander A. Myocardial infarction induces early increased remote ADAM8 expression of rat hearts after cardiac arrest. Scand J Clin Lab Invest 2011; 71: 553-562.
[15] Livak KJ and Schmittgen TD. Analysis of relative gene expression data using real-time quantitative PCR $2^{-\Delta\Delta Ct}$ method. Methods 2001; 25: 402-408.
[16] Mazzo FR, de Carvalho Frimm C, Moretti AI, Guido MC and Koike MK. Acute aortocaval fistula: role of low perfusion pressure and subendocardial remodeling on left ventricular function. Int J Exp Pathol 2013; 94: 178-187.
[17] Cerrudo CS, Cavallero S, Fermepin MR, Gonzalez GE, Donato M, Kouyoumdzian NM, Gelpi RJ, Hertig CM, Choi MR and Fernandez BE. Cardiac natriuretic peptide profiles in chronic hypertension by single or sequentially combined renovascular and DOCA-salt treatments. Front Physiol 2021; 12: 651246.
[18] Porter KE and Turner NA. Cardiac fibroblasts: at the heart of myocardial remodeling. Pharmacol Ther 2009; 123: 255-278.
[19] Chen HY, Zhou ZY, Luo YL, Luo Q and Fan JT. Knockdown of YKL-40 inhibits angiogenesis through regulation of VEGF/VEGFR2 and ERK1/2 signaling in endometrial cancer. Cell Biol Int 2021; 45: 2557-2566.
[20] Faibish M, Francescone R, Bentley B, Yan W and Shao R. A YKL-40-neutralizing antibody blocks tumor angiogenesis and progression: a potential therapeutic agent in cancers. Mol Cancer Ther 2011; 10: 742-751.